

2005

Dynamic Opto-VLSI lens and lens-let generation with programmable focal length

Zhenglin Wang
Edith Cowan University

Kamal Alameh
Edith Cowan University

Rong Zheng
Edith Cowan University

Salem Adherom

Follow this and additional works at: <https://ro.ecu.edu.au/ecuworks>



Part of the [Engineering Commons](#)

This is an Author's Accepted Manuscript of: Wang, Z. , Alameh, K. , Zheng, R. , & Adherom, S. (2005). Dynamic Opto-VLSI lens and lens-let generation with programmable focal length. Proceedings of Photonics Asia 2004. (pp. 138-142). Beijing, China. SPIE, Bellingham. Available [here](#)

Copyright 2005 Society of Photo-Optical Instrumentation Engineers (SPIE). One print or electronic copy may be made for personal use only. Systematic reproduction and distribution, duplication of any material in this paper for a fee or for commercial purposes, or modification of the content of the paper are prohibited.

This Conference Proceeding is posted at Research Online.

<https://ro.ecu.edu.au/ecuworks/2949>

Dynamic Opto-VLSI lens and lens-let generation with programmable focal length

Zhenglin Wang, Kamal E. Alameh, Rong Zheng and Selam Adherom
Centre for MicroPhotonic Systems, Electron Science Research Institute
Edith Cowan University, 100 Joondalup Drive, WA, 6027, Australia

ABSTRACT

In this paper we present and demonstrate a dynamic lens and lens array generation method with programmable focal length based on an Opto-VLSI processor. The Opto-VLSI is driven by computer generated algorithm to generate a discrete Fresnel lens phase hologram. By optimizing the phase hologram, lenses and lens arrays of different focal lengths ranging from 300mm to infinity can be realized. The optical axis of each lens element can be independently addressed to simultaneously focus and steer an optical beam within an angular range of $\pm 0.5^\circ$.

KEY WORDS: Opto-VLSI, wavefront generation, adaptive optics.

1. Introduction

Adaptive optics (AO) systems are currently employed in many optical applications to enhance imaging and quality of optical signals transmitted through optical systems [1]. Conventional AO systems use feedback mechanisms to sense wavefront distortions and programmable optical elements to compensate for these distortions in real-time. Recent advances in optical MEMS, computer-generated holography, and diffractive optics have enabled adaptive optics systems to be integrated in many applications such as infrared laser communication links, adaptive filtering for astronomical imaging, identification of targets for defense systems, retinal imagers, and optical microscopy. Several AO technologies have been demonstrated for different applications [2-7]. For real time wavefront correction, deformable mirrors (DMs), which are capable of changing the shape of their surface adaptively [2-4], and Liquid-Crystal Spatial Light Modulator (LC-SLM) have mostly been used. Although the use of deformable mirrors for wavefront error correction has become dominant in many AO applications, DM-based AO systems have many drawbacks, namely, (i) they require high-power actuators to mechanically steer a large number of reflecting mirrors (ii) bulky, (iii) expensive, and (iv) being mechanical elements, their lifetime is also limited. Conventional deformable mirrors normally need driving voltage over 100 V to achieve adequate mirror movement. LC-SLM provides an alternative technology with advantages of low cost, high reliability, compactness, easy control, low power consumption and high resolution. LC-SLMs have recently been used for different AO applications [5-7]. Vargas *et al.* [5] used a transmissive LC-SLM driven corrective element in an open-loop mode. The device had a bulk pixel design size (1mm x 1mm) that limited its spatial resolution. A solution to these obstacles is to phase wrap an optically addressed liquid-crystal spatial light modulator to extend its corrective range. Such a solution provides extremely high spatial resolution and an adequate temporal response for imaging applications [6].

In this paper we present and demonstrate an approach based on the use of Opto-VLSI processing to generate dynamic lens array with programmable focal lengths which can be potentially used for dynamic wavefront correction. An algorithm has been developed to generate diffractive Fresnel lenses with arbitrary displacement of their optical axes so that simultaneous beam focusing as well as steering is realized with focal lengths independently tunable from 300mm to infinity with an angular steering range of $\pm 0.5^\circ$.

2. Opto-VLSI spatial light modulator

Figure 1 shows a typical 8-phase Opto-VLSI processor, as well as the layout and structure of a single cell. The Opto-VLSI processor is an array of liquid crystal (LC) cells driven by a Very-Large-Scale-Integrated (VLSI) circuit that generates digital holographic diffraction gratings to steer and/or shape optical beams. Each pixel is assigned a few memory elements that store a digital value, and a multiplexer that selects one of the input voltages and applies it, through the aluminium mirror plate, across the LC cells. Indium-Tin Oxide (ITO) is used as the transparent electrode, and evaporated aluminium is used as the reflective electrode. The quarter-wave-plate (QWP) layer between the LC and the aluminium mirror is used to accomplish polarization-insensitive operation [8], [9]. Adaptive free-space beam shaping can be accomplished by driving the Opto-VLSI processor with appropriate phase-only holographic diffraction gratings.

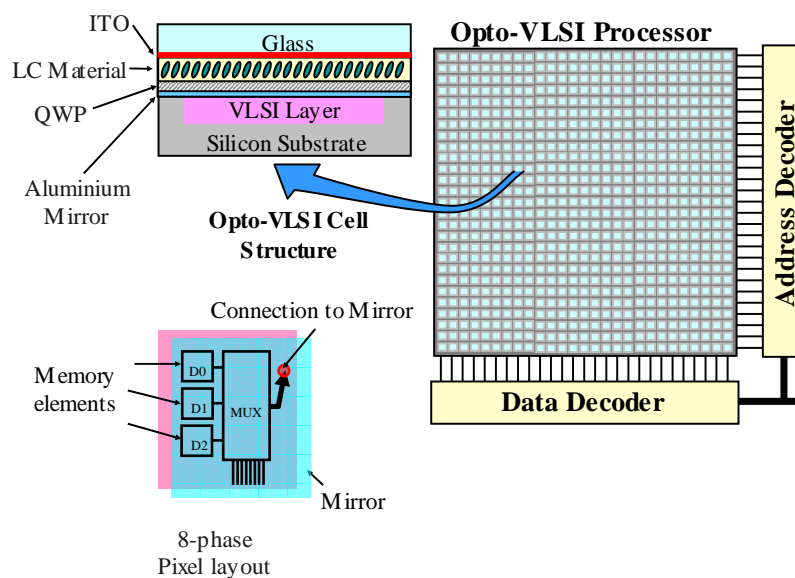


Figure 1. Opto-VLSI processor layout.

3. Algorithm

The Opto-VLSI processor is controlled by a computer generated hologram (CGH) using simulated annealing algorithm (SA) [10]. The simulated annealing algorithm for hologram generation first defines a cost function as a measure of the distance between the diffracted field pattern of the target T and the field pattern of the current candidate hologram. The target generally does not define the entire diffraction field, but rather a small subset of the diffracted field which is of interest. The algorithm, as formulated by Dames, et al. [10] starts from an initial random hologram pattern, $h(x,y)$ and computes the resulting diffraction field. The diffracted beam can be represented by a Fourier transform. For a pixellated hologram, $h(m,n)$, which represents the complex transmittance of each pixel (m, n) , the diffracted beam $H(k,l)$ is described by:

$$H(k,l) \equiv DFT\{h(m,n)\} \quad (1)$$

where (k,l) represents the coordinates in the output plane. Since the target intensity $T(k,l)$ is only defined at a few spots in the diffraction field, we then reduce the set $H(k,l)$ to a smaller set H_T containing only the coordinates where the target spots are defined. From this, we compute the cost function, which is a measure of the discrepancy between the target and the diffraction field of the hologram. One expression for the cost C is:

$$C = \sum \left\{ T(k,l) - |H_T(k,l)|^2 \right\}^2 \quad (2)$$

Next, a pixel or a group of pixels are randomly changed (subject to the constraint on the phase levels). Then the cost function is calculated again. However, the entire diffraction field $H(k,l)$ needs not be recalculated, it will be possible to compute ΔH_T arising from the change in a single pixel $\Delta h_{m,n}$:

$$H_T = \Delta h_{m,n} e^{-2\pi j(km+ln)/N} \quad (3)$$

This results in a change in cost, which is computed by equation (2). If the cost decreases (that is ΔC is negative), the pixel change(s) are accepted. Otherwise,, the pixels are accepted with a probability of $e^{\Delta C/T}$, where T is the "temperature", which is gradually reduced as the number of iterations increases. The decrease in temperature can be expressed as:

$$T = T_o e^{-T_e i/I} \quad (4)$$

where T_o and T_e are parameters that determine the starting value and rate of decrease of the temperature, i is the current iteration number, and I is the total number of desired iterations. The end of the algorithm can be set at a certain number of iterations, or when the cost has been reduced to a determined level, or alternatively, when the temperature has been reduced to a certain value. Figure 2 shows the flow chart for the simulated annealing algorithm used in this work.

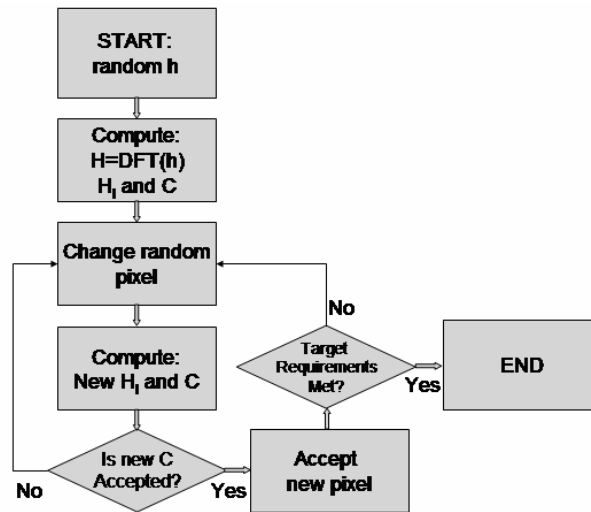


Figure 2. Flowchart for simulated-annealing-based hologram generation.

A Fresnel lens hologram can simply be generated by driving the Opto-VLSI processor with a discrete spherical wavefront. Therefore, the phase distribution for a Fresnel lens of focal length f is given by

$$\phi(x, y) = \exp \left\{ -2\pi \text{mod} \left(\frac{x^2 + y^2}{\lambda f} \right) \right\} \quad (5)$$

where $\phi(x,y)$ is the complex phase distribution in the two spatial dimensions, λ is the optical wavelength. The modulus function ensures that the phase remains between 0 and 2π . Note that, since the Opto-VLSI processor has a limited number of phase levels within the range of 0 and 2π , only phases that are rounded to the nearest available discrete levels can drive the hologram.

4. Experimental results

Figure 3 shows the experimental setup used to demonstrate the concept of dynamic Opto-VLSI lens. The Opto-VLSI processor is a 128×128 -pixel, 40-micron pitch nematic liquid crystal (fill factor $\sim 60\%$). The input fiber with a collimator has 1mm output beam size. The beam was expanded to about 5 mm by a telescope expander so that it filled most of the Opto-VLSI working area [11]. Different Fresnel lens holograms were generated to control the Opto-VLSI processor and the output beam profiles were imaged by an imaging lens and captured by CCD camera. Our aim in the experiments was

to prove the concept of the dynamic Opto-VLSI lens by focusing the input optical beam by means of discrete phase distribution.

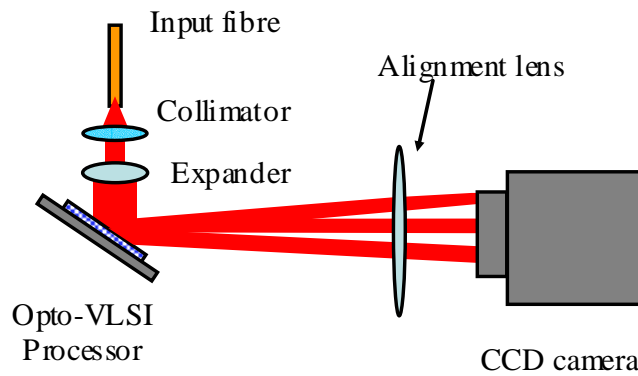


Figure 3. Dynamic lens/lenslet wave-front generation.

Figure 4(a)-(c) show the measured output beam profiles and corresponding single Fresnel lens holograms of different focal lengths. By uploading different optimized Fresnel lens holograms, the output beam size was reduced by reducing the focal length of the Fresnel hologram. In Figure 4(d), the centre of the Fresnel lens was shifted so that beam steering is added to the focusing capability of the Opto-VLSI processor. Note that in Figure 4(d) the beam captured by the CCD moved upward as the centre of the Fresnel lens moved downward. This image inversion is caused by an imaging lens placed in front of the CCD camera. The measured focal length dynamic range was from 300 mm to infinity and the maximum steering angle was $\pm 0.5^\circ$ using 8-level phase holograms.

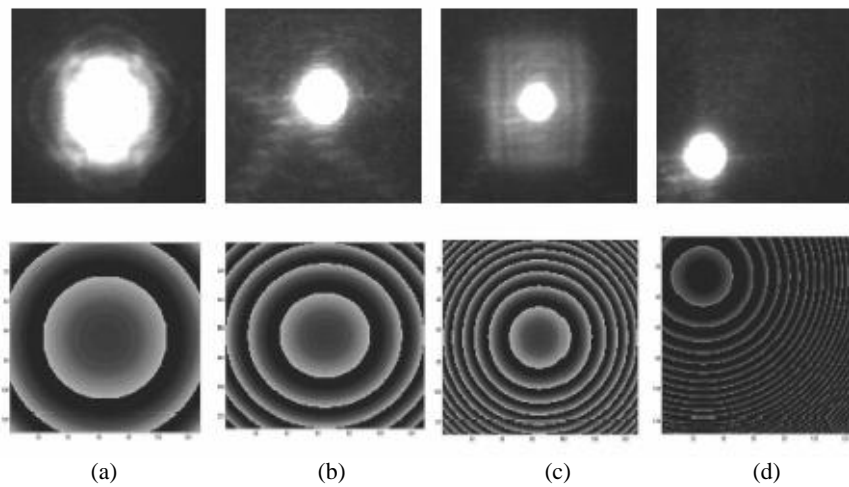


Figure 4. Output beam profile and corresponding single Fresnel lens hologram images

Figure 5 illustrates the capability of the Opto-VLSI processor to synthesize adaptive lens arrays, where various beam profiles captured by a CCD camera are displayed. These profiles were generated by driving the Opto-VLSI processor with an array of discrete Fresnel lens holograms, which are also displayed in Figure 5. It is noticeable that for each Fresnel lens element the dimension, centre and phase distribution can independently be adjusted. This capability provides an efficient wavefront compensation method when combined with wavefront sensor lens array. The inherent phase discontinuity of the Opto-VLSI processor results in unwanted noise in the surrounding of the focused beam. However, this noise can significantly be reduced by using a smaller pixel size ($10 \mu\text{m}^2$ is currently feasible) and larger number of discrete phase levels (eg. 256).

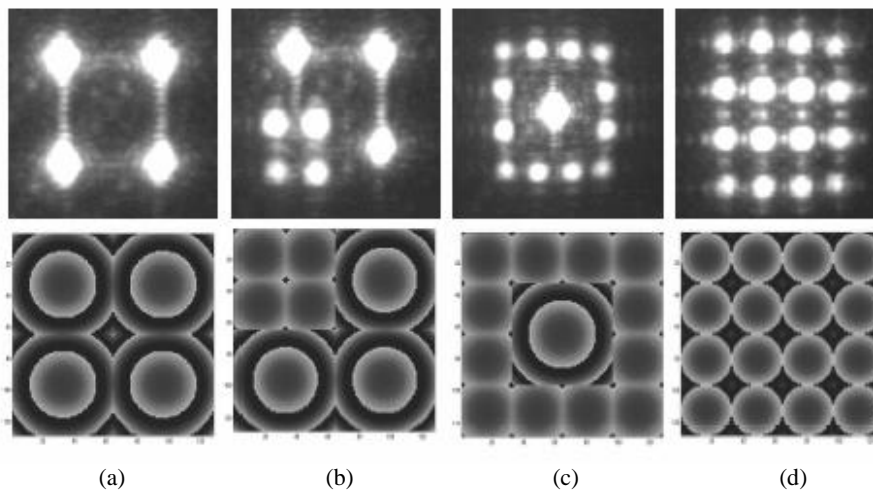


Fig. 5 Output beam profiles and related lenslet Fresnel lens hologram images

5. Conclusions

In conclusion, the use of reconfigurable Opto-VLSI processors for adaptive optical wavefront correction has been presented and its feasibility for generating arbitrary Fresnel lens arrays has been demonstrated. Different examples of lens arrays were realized for dynamic wavefront correction where the focal lengths and optical axes of the lens array elements were independently controlled. The measured focal length dynamic range was from 300mm to infinity, and the maximum beam steering angular range was $\pm 0.5^\circ$. New advances in electro-optic materials and VLSI design and processing will enable the fabrication of cost-effective and practical polarization-insensitive Opto-VLSI processors for many AO applications. An Opto-VLSI processor in conjunction with a Hartmann-Shack wavefront sensor can provide a simple method to compensate for wavefront error in adaptive optics systems

REFERENCES

1. R.K.Tyson, *Principales of Adaptive Optics* (ACADEMIC, New Yoke, 1991).
2. A. W. Dreher, J. F. Bille, and R. N. Weinreb, *Appl. Opt.* **28**, 804 (1989).
3. J. Liang, D. R. Williams, and D. T. Miller, *J. Opt. Soc. Am. A* **14**, 2884 (1997).
4. Bifano, T. G., Perreault, J. A., and Bierden, P. A., "Micromachined deformable mirror for optical wavefront compensation," *Proc. SPIE Vol. 4124*, p. 7-14, 2000.
5. John D. Gonglewski, Mikhail A. Vorontsov, Mark T. Gruneisen. "High-Resolution Wavefront Control: Methods, Devices, and Applications II"; Eds., Nov 2000.
6. F. Vargas-Martin, P.M. Prieto and P. Artal, (1998). Correction of the aberrations in the human eye with a liquid-crystal spatial light modulator: limits to performance. *J. Opt. Soc. Am. A*, **15**, 2552-2562, 1998.
7. G. D. Love, "Wave-front correction and production of Zernike modes with a liquid-crystal spatial light modulator," *Appl. Opt.* **36**, 1517-1524 (1997).
8. Ahderom, S., Raisi, M., Alameh, K.E., and Eshraghian, K., "Adaptive WDM equalizer using Opto-VLSI beam processing", *IEEE Photon. Technol. Lett.*, Vol. 15, No. 11, pp. 1603- 1605, 2003.
9. Crossland, W.A., Wilkinson, T., Manolis, I., Redmaond, M. and Davey, A. "Telecommunications applications of LCOS devices", In proceedings, *9th International Topical Meeting on Optics of Liquid Crystals, OLC 2001*, 2001.
10. M.P. Dames, R.J. Dowling, P. McKnee, and D. Wood. Efficient optical elements to generate intensity weighted spot arrays: design and fabrication. *Applied Optics*, 30(19):2685-2691, July 1991.